Relationship between SW velocity and muscle activation is inconsistent across different muscle types

Michel Bernabei[1,5]
Thomas G. Sandercock[2]
Eric J. Perreault[1,4,5]
Sabrina S. M. Lee[3]

[1]Department of Biomedical Engineering, Northwestern University, Evanston, IL

[2]Department of Physiology, Northwestern University, Evanston, IL

[3]Department of Physical Therapy and Human Movement Sciences, Northwestern University, Chicago, IL

[4]Department of Physical Medicine and Rehabilitation, Northwestern University, Evanston, IL

[5]Shirley Ryan AbilityLab, Chicago, IL

* Corresponding author
Sabrina S.M. Lee
625 N Michigan Avenue
Suite 1100
Chicago, IL 60611
s-lee@northwestern.edu

ABSTRACT

There is an increasing use of shear wave ultrasound elastography to quantify material properties of muscles under various conditions such as muscle length, levels of activation, in healthy and pathological muscle. However, little is known about the variability in shear wave velocity among muscles. The purpose of this study was to assess the variability of the relationship between SWV and activation across muscles with different architecture, specifically pennation angle: biceps brachii (parallel), tibialis anterior (moderately pennate), gastrocnemius (highly pennate). We tested these muscles at matching levels of activation and similar muscle lengths, relative to optimal length, to limit differences in force across muscles. Shear wave velocity-squared increased with higher levels of muscle activation ($p<0.001$), but the relationship between shear wave velocity-squared and activation was different across all three muscles ($p<0.001$). This indicates that SWV was inconsistent across muscle types, even when considering similar levels of activation and torque production. Under passive conditions, shear wave velocity-squared covaried with muscle length and was different across muscles ($p<0.001$), even at shortest lengths, when differences due to passive force were minimal. Variation of shear wave velocity-squared was only partially explained by changes in pennation angle during contraction ($p = 0.004$, $R^2 = 0.4$). Our findings suggest that the shear wave velocity varies across muscles under passive and active conditions even when relative length is considered and that shear wave velocity may be dependent on other muscle properties, other than pennation angle, that are different between the three muscles.

INTRODUCTION

Shear wave ultrasound elastography can be used to estimate the mechanical properties of muscles by measuring the velocity of propagation of SWs; these waves propagate faster in stiffer muscles and in muscles under tension. Previous research has shown high inter-session and inter-operator repeatability of SW measurements in passive (Koo et al. 2013; Lacourpaille et al. 2012) and active (Lapole et al. 2014; Yoshitake et al. 2014) conditions when controlling for muscle level of activation and length, justifying a systematic assessment using shear wave ultrasound elastography of human muscles already underway (Le Sant et al. 2017, 2018). However, the remarkable differences in anisotropy of muscle tissues and the muscle-specific characteristics of activation and length-dependent tensional changes challenge the ability of ultrasound to produce consistent and accurate estimates of SW velocity (SWV) across muscles.

We have previously shown that short-range stiffness of cat muscles vary linearly with force and in a similar fashion across muscles with different architectures (Cui et al. 2008). This suggests that SWV might be constant across muscles if activation and sarcomere length are the same, as a change in passively or actively generated forces would alter SWV proportionally (Bernabei et al. 2017; Eby et al. 2013). In contrast, measures obtained across different muscle types seem to vary substantially under passive conditions (Dubois et al. 2015; Le Sant et al. 2017; Xu et al. 2016), suggesting a muscle-specific relationship between SWV and muscles' mechanical properties.

We hypothesize here that such variability of SWV could be explained by architectural and morphological differences between muscle types. First, architectural variations caused by differences in pennation angle, fiber length and the presence of stiffer aponeuroses can lead to muscle-specific differences in the stress-strain relationship during active contractions (Azizi and Deslauriers 2014; Blemker et al. 2005). Supporting this idea, Koo et al. (2013) showed a partial correlation between SWV and architectural parameters, such as cross-sectional area and muscle mass, in passive muscle. Second, estimates of SWV can be related to a unique descriptor of mechanical properties of tissues, such as shear modulus, if measurements are made along the fibre direction (Gennisson et al. 2010; Royer et al. 2011). Measurements made with small deviations from the fiber direction, described here as probe-fascicle angle which result from pennation angles and changes in pennation angle upon activation, have been suggested to be potentially inaccurate (Herzog 2017). In addition, an interesting complication is given by differences across muscles in the relative use of recruitment in the force generation process (Hodson-Tole and Wakeling 2007; Lawrence and De Luca 1983); for similar levels of force within a muscle compartment can be obtained by recruiting some fibers at high stiffness or many at lower stiffness. In conclusion, comparing SWV across different muscles is non-trivial and may lead to substantial, unexplained variability which may mask the effects of changes in a muscle' mechanical properties.

This study aims at assessing the variability of the relationship between SWV and activation across muscles with different architecture, specifically pennation angle:

biceps brachii (parallel), tibialis anterior (moderately pennate), gastrocnemius (highly pennate). We tested these muscles at matching levels of activation and similar muscle lengths, relative to optimal length, to limit differences in force across muscles. We hypothesized that the dependency of SWV on these parameters will be independent of muscle. In testing this hypothesis, we also expect to reveal what can be considered normal inter-muscle variability when using SWE to estimate muscle mechanical properties in humans.

METHODS

Subjects

Twelve healthy young adults took part in this study (7 females and 5 males, mean (SD) age: 29 (5) years; height: 1.72 (0.11) m; body mass: 73.7 (14.2) kg). Subjects had no history of major orthopedic diagnosis, musculoskeletal trauma, or persistent joint pain at the targeted body locations. All experimental procedures were approved by Northwestern University's Institutional Review Board (#0020-33-96), in compliance with the Helsinki Declaration. All subjects received and signed informed consent prior to collecting data.

Setup & protocol

Participants were asked to sit upright on a Biodex (Biodex Medical Systems Inc., Shirley, USA) chair. Their dominant forearm or lower leg was secured in neutral position with a fiberglass cast to minimize activity of unrecorded muscles and standardize wrist and ankle joint positions. The cast was then secured to a metal plate attached to the

shaft of the Biodex motor and aligned to its rotational axis (e.g. Fig. 1A). Three different muscles were targeted in separate sessions: i) the long head of the biceps brachii (BB), ii) medial gastrocnemius (MG) in the posterior crural triceps surae muscle group and iii) tibialis anterior (TA) in the anterior crural compartment. These muscles were chosen because of their remarkably different architectural features (Table 1). Participants were instructed to contract the muscle of interest while ultrasound, torque, and electromyography (EMG) data were simultaneously collected. EMG data provided the subject with an online activity feedback to control the level of muscle activation. For each different muscle, passive and maximum voluntary contraction (MVC) trials were performed at the beginning of each session; then a minimum of 30 trials were recorded with increasing levels of muscle activation from 5% to 50%MVC in 5%MVC steps. We manipulated muscle length through changing joint angle configuration; isometric voluntary contractions performed at various muscle activity levels were repeated with elbow or ankle joint positioned at three different angles based on literature ranges for the muscles of interest (Leedham and Dowling, 1995; Maganaris, 2001; Maganaris, 2003): 100-110-120° for BB, 35-45-55° for TA, maximum dorsiflexion to +5° and +10° plantarflexion for MG (Fig. 1B) (Maganaris 2001, 2003; Kawakami et al., 2002). The imposed joint angles were adjusted to individual subject based on their comfortable range of motion. Angles at adjacent joints (knee, hip, shoulder) affecting the muscle of interest were recorded and held constant throughout data collection. Anthropometry data of upper and lower extremities, as well as distances between load cell and joint centers of rotation, were recorded during each measurement session. Trials were randomized across levels of muscle activation and imposed joint angles.

Joint torques resulting from isometric contractions were measured with a six degrees of freedom load cell (moment range: ± 76.3 Nm, accuracy 0.05 N, JR3 Inc., Woodland, USA), attached to the biodex motor shaft used here for position control. Surface EMG signals via bipolar electrodes (#272, Noraxon, USA) placed on the targeted muscles were provided to the subject as an online feedback for controlling muscle activity levels during data collection. In addition, EMG was recorded from synergistic (soleus) and antagonistic (triceps brachii, MG and TA) muscles to account for effect of co-activation. An experienced investigator identified the muscles of interests and placed the electrodes for all subjects. EMG signals were amplified to maximize signal resolution for each channel (x100 to x1000, Bagnoli EMG system, Delsys Inc., Boston, MA) and band-pass filtered (20-450Hz band-pass, IV-order Butterworth) before further analysis. The online EMG feedback provided to the subject was additionally low-pass filtered (1Hz low-pass, II-order Bessel). EMG, load cell and ultrasound trigger signals were sampled (2 kHz) and digitized with a 16-bit data acquisition board (USB-6343, National Instruments, Austin, US).

Ultrasound measurements

The ultrasound transducer was secured on the muscle of interest with a neoprene custom-molded holder and positioned at the mid-belly region of BB and at the proximal region of MG and TA muscle bellies. The imaging plane was aligned with the fascicle plane as viewed from the B-mode image. The region for elastography was a 25x10 mm rectangle between the superficial and deep aponeuroses (Fig. 2A). For each isometric contraction a B-mode ultrasound image and a SW propagation video were

simultaneously captured using a research grade ultrasonography system (Aixplorer SuperSonic Imagine, Aix-en-Provence, France) equipped with a 256 elements linear transducer array (4-15 MHz, SuperLinear 15-4, Vermon, France). The parameters of the system were set to i) mode: MSK – foot and ankle ii) opt: std iii) persist: no, to maximize the sampling rate and avoid bias due to locked proprietary data post-processing. The software on our system provides SW movie data sampled at 8 kHz in sequences of 42 frames for each acoustic radiation pulse, recorded simultaneously with a single B-mode ultrasound image.

Data analysis

Torque and EMG data. Signals were averaged over a 450 ms time-window prior to the onset of ultrasound data recording. Torque data were low-pass filtered (IV-order Butterworth, 20Hz) and expressed relative to the joint center of rotation. Only torques in the sagittal plane, the dominant rotational plane for elbow and ankle joints, were considered for further analysis. Magnitude of rectified, filtered EMG data was normalized and expressed as a percentage of the MVC value recorded in each measurement session. Co-activation of synergists and antagonists was assessed as the ratio between the root-mean-square (RMS) value of the EMG signal during contraction and at rest. Crosstalk between electrodes placed in adjacent muscles was assessed with a normalized cross-correlation index (Winter et al., 1994). Trials with co-activation ratios higher than 5 SD compared to passive state and negligible crosstalk index were discarded.

We compared SWV data across muscles by matching joint angle configurations yielding the maximum rate of torque increase for several reasons: i) the length-force relationship of human muscles may vary in vivo across different muscles and for the same muscle across different subjects (Narici et al., 2016; Winter and Challis, 2010); and ii) SWV covaries with the level of passive and active muscle tension (Bouillard et al., 2011; Koo and Mak, 2005), First, the slope of the torque-EMG relationship was compared across the three imposed joint angle configurations for each muscle and subject (Fig. 2C). Then, ultrasound data relative to the joint angle configuration corresponding to the steeper slope was selected for further analysis.

Ultrasound data

B-mode images showing the underlying tissue organization were used to select the region of interest for calculating the velocity of propagation of SWs; a similar muscle region was selected for each muscle type, avoiding areas near aponeuroses and with recurrent fat tissue inclusions (Fig. 2A). Each pixel $d(x,z,t)$ in the movie frame shows the tissue displacement over a lateral distance *x*, a focal depth *z* and time *t*. The displacement data from each frame was averaged across a depth of 8.5 mm in the *z* dimension to improve signal-to-noise ratio. SWV was estimated from the averaged data using a time-to-peak method (34) over a lateral distance (*x*) up to 20 mm from the remotely induced pressure source. We reported here direct estimates of SWV instead of the more commonly reported shear or Young's moduli because muscle anisotropy violates the assumption made on the theoretical relationship between shear and Young's moduli for simple materials (Royer et al., 2011). In addition, there is enough

183 evidence to suspect that SW propagation depends not only on tissues' intrinsic
184 stiffness, but also on the stress imposed on the tissue, which in muscle and tendons
185 might be the dominant factor (Bernabei et al., 2017; Martin et al., 2018). However, since
186 there is a known proportionality between muscle stress, shear modulus and the square
187 of SWV, we reported most of our results in terms of SWV squared.
188
189 *Muscle architecture data*
190 In each position, probe-fascicle angle and fascicle length were extracted from ultrasonic
191 images of the targeted muscles. Probe position was adjusted by visualizing the fascicles
192 along their lengths from the superficial to deep aponeuroses, as a proof that the
193 ultrasonogram was parallel to fascicles (Kawakami et al., 1998). Probe-fascicle angle
194 (□) was defined as the angle between a fascicle within the imaged muscle region and
195 the region of interest for elastography provided by the AIXplorer in the DICOM image
196 (Fig. 2A, color map rectangle). This angle is useful to assess effects of orientation of the
197 probe in respect to muscle fibers, which results from differences in pennation angle
198 across muscles and from activation. In the MG only, the fascicle length was estimated
199 by tracing the same fascicle from the superficial aponeurosis to the deep one. Images
200 were pre-processed to enhance contrast of the features of interest, while tracking was
201 standardized using a Matlab user interface. All architectural measurements were
202 completed by a single operator; the known reproducibility of this measure (Kawakami et
203 al., 1998) was confirmed here by a correlation coefficient of 0.997 across three repeated
204 measurement sessions over subsequent days, on all probe-fascicle angle data from the
205 same muscle (30 samples x 3 days).

Statistics

Linear mixed-effects models were used for all hypothesis tests. Our primary hypothesis that SWV is consistent across muscle types was tested by modeling the activation-dependent changes in SWV occurring in each muscle in passive and active conditions, separately. For each model, EMG and SWV squared were considered as continuous variables, muscle and joint angle configuration as fixed effects and subject as a random effect. To test the hypothesis that the relationship between SWV squared and EMG is independent of muscle architecture we used a generalized linear model in which EMG in the target muscle was considered as a continuous factor, muscle type a fixed factor, and each subject as a random factor. SWV and torque were treated as continuous dependent variables. A first model was used to test for effects of activation, joint angle configurations and their interaction on torque magnitudes (e.g. Fig. 2B). A second model considered muscle activation together with muscle type and their interaction to predict SWV squared values under active conditions (e.g. Fig. 3A). A third model was used to test for effects of different muscle types on SWV-squared under passive conditions (Fig. 4). A fourth model tested the effects of probe-fascicle angle with activation level on SWV in active muscle (Fig. 5). All models assumed a random intercept for subject as a grouping variable. An ANOVA was used to test model significance and the overall significance of each modeled predictor. Significance was assessed at the $p < 0.05$ level. All statistical tests, as well as all signal and image processing, were performed in matlab (Mathworks, Natick, USA).

RESULTS

Effects of activation and joint angle on net joint torque

Joint torque covaried with muscle activation and its rate of change was different across the imposed joint angle configurations (e.g. Fig. 2B). The average variation across joint angles was 0.24 Nm*%MVC^{-1} for BB, 1.17 Nm*%MVC^{-1} for MG and 0.44 Nm*%MVC^{-1} for TA. This was evaluated on BB, MG, and TA independently, considering EMG as a continuous factor, joint angle as a fixed factor and subject as a random factor. For each muscle, a linear model accounting for differences in torque-EMG relationship across the imposed joint angles explained a larger portion of variability than one considering effects of activation only ($p < 0.05$ for all muscles, R^2 increased by 0.8%). For further analysis, we selected only those trials associated with the maximum rate of change for joint torque. The implicit assumption is that the highest rate of force generation will be associated with muscle lengths near the steepest length-force relationship curve, which allows comparison of SWV estimates across muscles with similar force levels relative to cross-sectional area.

Effects of activation on SW velocity across muscles

SWV-squared increased with progressively higher levels of muscle activation from 5 % to 50 %MVC ($F = 128.7$, $df1 = 1$, $df2 = 905$, $p < 0.001$, $R^2 = 0.871$; e.g. Fig. 3A). This was tested with a linear mixed-effects model predicting SWV^2 by modeling muscle activation (%MVC) as a continuous factor, muscle type as a fixed categorical factor and subject as a random factor. Contrary to our null hypothesis, the relationship between SWV squared and activation was different across muscles ($F = 19.7$, $df1 = 2$, $df2 = 905$,

$p < 0.05$, $R^2 = 0.87$), BB and MG generally showing a lower slope compared to TA, respectively 2.95, 2.48 and 4.79 $(m^2/s^2)*(\%MVC)^{-1}$ (Fig. 3B). Conversely, average values of SWV^2 were drastically lower in MG (28.7 ± 13.5 m^2/s^2) with respect to TA (123.7 ± 49.0 m^2/s^2) and BB (106.0 ± 39.7 m^2/s^2). This indicates that SWV was inconsistent across muscle types, even when considering similar levels of activation and torque production.

Effects of muscle length on SW velocity under passive conditions

Under passive conditions, measures of SWV squared collected at four different joint angles increased proportionally from shorter to longer muscle lengths (Fig. 4, $F = 3.47$, $p = 0.016$). Such increase differed across muscles ($F = 41.3$, $p < 0.05$, $R^2 = 0.80$): the smallest variation was observed in the biceps (3.85 ± 6.5 m^2/s^2), while the gastrocnemius had the largest increase (30.4 ± 17.4 m^2/s^2) across the whole range of imposed joint angles. This was evaluated with a linear mixed-effects model including muscle type and joint angle configuration as categorical fixed factors, while subject was a random factor. Absolute values of SWV squared were substantially different across muscles in passive conditions even at their shortest lengths (Fig. 4A 'short', $F = 33.08$, $d1 = 2$, $d2= 183$; $p < 0.05$), where we expected differences due to passive muscle tension to be minimal. The slowest waves were observed in the BB (3.1 ± 0.5 m^2/s^2) and the fastest waves in the TA (10.0 ± 7.7 m^2/s^2); note that at the shortest length, variability of SWV in passive conditions was twofold in the TA (SD: 7.7 m^2/s^2) compared with BB and MG (SD: 0.5 m^2/s^2, 3.0 m^2/s^2, respectively). These results show that velocity of propagation of SWs covaries with changes in muscle length. However, such

covariation was inconsistent across different muscle types, seemingly showing larger variation for muscles with higher pennation angle.

Effect of the angle between ultrasound probe and fascicle orientation on SWV

Variation of SWV across different activation levels was partially associated with changes in the probe-fascicle angle in MG (0.05 (m/s)*deg^{-1}, $F = 7.22$, $p = 0.007$) and TA (1.01 (m/s)*deg^{-1}, $F = 4.25$, $p = 0.039$), while such angle was virtually zero for all applied conditions in BB (Fig. 5). This was tested independently for each muscle by a linear mixed-effects model considering activation as a fixed factor, probe-fascicle angle as a continuous factor and joint angle nested within each subject as random factor. Not surprisingly, the probe-fascicle angle was also highly correlated with activation in MG (1.01 deg*10%MVC^{-1}, $F = 439.21$, $df1 = 1$, $df2 = 936$, $p < 0.05$) and TA (0.10 deg*10%MVC^{-1}, $F = 21.99$, $df1 = 1$, $df2 = 974$, $p < 0.05$). Thus, these results show that activation and pennation angle changes affect SWV data independently in MG and TA, but their individual contributions could not be quantified due to covariation between probe-fascicle angle and muscle activation.

DISCUSSION

This study shows that human muscles with remarkably different architecture produce substantially different estimates of SWV, even when comparing between conditions with similar levels of passive and relative active muscle tension. In addition, differences in the ultrasound probe-fascicle angle due to pennation angle and pennation angle changes upon activation were investigated as a co-determinant of SWV variability, but only a small effect was found.

Previous experiments in humans have assessed SWV in muscle tissues by controlling the joint angle spanned by the target muscles (Maïsetti et al. 2012; Le Sant et al. 2017), the level of joint torque (Lapole et al. 2014) or passive muscle force (Koo et al. 2013). These studies have observed that SWV in individual muscles vary with the extent of expected passive and active muscle tension. However, when comparing different human muscles with similar levels of passive and active tension, we found substantial differences in the average estimates of SWV. While it is not surprising that SWV increased with higher levels of activation, the average SWV and its rate of increase varied drastically between BB, MG and TA in active conditions. Under passive conditions, the average measure and rate of variation of SWV with changing muscle length, obtained by adjusting the joint angle spanned by the target muscle, was also different across the same muscles. Interestingly, the rate of increase of SWV over increasing joint angles was qualitatively consistent with the differences in pennation angle at rest across these muscles: biceps brachii (parallel), tibialis anterior (moderately pennate), gastrocnemius (highly pennate). Thus the question: is the increase in muscle

315 tension obtained by passive stretching steeper in pennated muscles? Note that SWV
316 was still different when comparing these muscles at small joint angles yielding virtually
317 no joint torque. If the effect of passive tension was limited, persisting variation in the
318 wave speed may indicate differences in intrinsic stiffness across muscle types, or,
319 alternatively, an effect of misalignment between ultrasound probe and fascicle
320 orientation.
321
322 These results suggest that considering only changes in active and passive tension as
323 determinant of SWV across muscles is not sufficient. This discrepancy could be
324 effectively explained by differences in the intrinsic relationship between SWV, force and
325 stiffness between muscles. However, this hypothesis is in contrast with measures in cat
326 muscles showing that the stiffness-force relationship is remarkably similar across
327 muscle types (Cui et al. 2008). As an alternative explanation, we hypothesized that
328 architectural differences across muscles could affect SW propagation, thus the estimate
329 of SWV obtained with ultrasound. Supporting this idea is previous work in humans in
330 vivo (Gennisson et al. 2010; Maïsetti et al. 2012) and in animal specimens (Eby et al.
331 2013), which has shown that the effect of the orientation of the probe on SWV within a
332 muscle was substantial when the insonification plane was not aligned with the plane of
333 the muscle fascicles. The higher the degree of misalignment, the lower the average
334 SWV estimate. In this skewed configuration, only portion of the muscle fascicle is visible
335 in the b-mode image. Because pennation angle varies across muscles and during
336 activation, investigators are aware that the orientation of the probe in respect to muscle
337 fascicles can change between different muscles and even between different regions of

the same muscle. Online adjustments of probe orientation allow to correct for such changes, but optimal alignment in muscles with complex architecture, such as MG and TA, is complicated by out of plane fiber curvature. A titling angle within the plane of the fascicles, mimicking the effects of changes in fibers pennation in a single plane, showed small effects (<1.3 % for an angle of max 20°; Miyamoto et al. 2015) in the parallel-fiber BB. In our experiment, we observed that some residual variability of SWV was associated with changes in pennation angle upon activation in TA and MG. Note that we limited our analysis to angles in the insonification plane, so that this result might underestimate the effect of 3D misalignment on wave propagation.

CONCLUSIONS

Our results demonstrate that the variation of SWV across different muscle types cannot be accounted for by passive and active changes in muscle tension alone. We also showed that the angle between probe orientation and muscle fascicles given by pennation can only partially explain such discrepancy. The factors determining SWV variation should be clarified before comparing estimates of muscle mechanical properties provided by ultrasound across different muscle types.

Note that we calculated an indirect estimate of active tension by measuring EMG and by characterizing torque-EMG relationship for each target muscles. We also assumed that the relationship between passive tension and joint angle would be similar across muscle types. Future studies providing direct measures of tension and stiffness as well as a

measure of 3D probe-fascicle angle would be helpful to clarify SWV dependency on mechanical and architectural factors that differ across muscle types.

ACKNOWLEDGMENTS

The authors thank Daniel Ludvig for contributions to statistical analysis and Allison Bingqing Wang and Kristen Jakubowski for the preliminary analysis of ultrasound elastography images.

GRANTS

This study was supported by National Institute of Health Grant 5R01-AR-071162-02 to E. J. Perreault.

DISCLOSURES

No conflicts of interest, financial or otherwise, are declared by the authors.

AUTHOR CONTRIBUTIONS

S.S.M.L., E.J.P., and T.G.S. conceived and designed research; M.B. and S.S.M.L. performed experiments; M.B. analyzed data; M.B., S.S.M.L., E.J.P., and T.G.S. interpreted results of experiments; M.B. prepared figures; M.B. drafted manuscript; M.B., S.S.M.L., E.J.P., and T.G.S. edited and revised manuscript; M.B., S.S.M.L., E.J.P., and T.G.S. approved final version of manuscript.

REFERENCES

Azizi E, Deslauriers AR. Regional heterogeneity in muscle fiber strain: The role of fiber architecture. *Front Physiol* 5 AUG: 1–5, 2014.

Bernabei, M., Lee, S. S. M., Perreault, E. J. and Sandercock, T. G. (2017). Decoupling stiffness and tension in the active muscle : effects on SW propagation.pp. 1–2.

Blemker SS, Pinsky PM, Delp SL. A 3D model of muscle reveals the causes of nonuniform strains in the biceps brachii. *J Biomech* 38: 657–665, 2005.

Bouillard, K., Nordez, A. and Hug, F. Estimation of individual muscle force using elastography. *PLoS One* 6, 2011.

Cui L, Perreault EJ, Maas H, Sandercock TG. Modeling short-range stiffness of feline lower hindlimb muscles. *J Biomech* 41: 1945–1952, 2008.

Dubois G, Kheireddine W, Vergari C, Bonneau D, Thoreux P, Rouch P, Tanter M, Gennisson JL, Skalli W. Reliable Protocol for SW Elastography of Lower Limb Muscles at Rest and During Passive Stretching. *Ultrasound Med Biol* 41: 2284–2291, 2015.

Eby SF, Song P, Chen S, Chen Q, Greenleaf JF, An KN. Validation of SW elastography in skeletal muscle. *J Biomech* 46: 2381–2387, 2013.

Gennisson JL, Deffieux T, Mace E, Montaldo G, Fink M, Tanter M. Viscoelastic and anisotropic mechanical properties of in vivo muscle tissue assessed by supersonic shear imaging. *Ultrasound Med Biol* 36: 789–801, 2010.

Herzog W. Skeletal muscle mechanics: questions, problems and possible solutions. *J Neuroeng Rehabil* 14: 98, 2017.

Hodson-Tole EF, Wakeling JM. Variations in motor unit recruitment patterns occur within and between muscles in the running rat (Rattus norvegicus). *J Exp Biol* 210: 2333–45, 2007.

Kawakami, Y., Ichinose, Y., Fukunaga, T., Rana, M., Hamarneh, G., Wakeling, J. M., Farcy, S., Nordez, A., Dorel, S., Hauraix, H. Architectural and functional features of human triceps surae muscles during contraction. 398–404, 1998).

Koo TK, Guo JY, Cohen JH, Parker KJ. Relationship between shear elastic modulus and passive muscle force: An ex-vivo study. *J Biomech* 46: 2053–2059, 2013.

Lacourpaille L, Hug, F, Bouillard K, Hogrel J. Supersonic shear imaging provides a reliable measurement of resting muscle shear elastic modulus. *Physiol Meas*, 33 (3), N19-28, 2012.

Lapole T, Tindel J, Galy R, Nordez A. Contracting biceps brachii elastic properties can be reliably characterized using supersonic shear imaging. *Eur J Appl Physiol* 115: 497–505, 2014.

Lawrence JH, De Luca CJ. Myoelectric signal versus force relationship in different human muscles. *J Appl Physiol* 54: 1653–1659, 1983.

Leedham, J. S. and Dowling, J. J. Force-length, torque-angle and EMG-joint angle relationships of the human in vivo biceps brachii. *Eur. J. Appl. Physiol. Occup. Physiol.* 70, 421–426, 1995.

Maganaris, C. Force-length characteristics of in vivo human skeletal muscle. *Acta Physiol. Scand.* 172, 279, 2001.

Maganaris, C. N. (2003). Force-Length Characteristics of the In Vivo Human Gastrocnemius Muscle. *Clin. Anat.* 215–223, 2003.

Maïsetti O, Hug F, Bouillard K, Nordez A. Characterization of passive elastic properties of the human medial gastrocnemius muscle belly using supersonic shear imaging. *J Biomech* 45: 978–84, 2012.

Miyamoto N, Hirata K, Kanehisa H, Yoshitake Y. Validity of measurement of shear modulus by ultrasound SW elastography in human pennate muscle. *PLoS One* 10: 1–11, 2015.

Martin, J., Brandon, S., Keuler, E., Hermus, J., Ehlers, A., Segalman, D., Allen, M. and Thelen, D. Gauging force by tapping tendons. *Nat. Commun.* 2–10, 2018.

Narici, M., Franchi, M. and Maganaris, C. Muscle structural assembly and functional consequences. *J. Exp. Biol.* 219, 276–284, 2016.

Royer, D., Gennisson, J.-L., Deffieux, T. and Tanter, M. On the elasticity of transverse isotropic soft tissues (L). *J. Acoust. Soc. Am.* 129, 2757–2760, 2011.

Le Sant G, Nordez A, Andrade R, Hug F, Freitas S, Gross R. Stiffness mapping of lower leg muscles during passive dorsiflexion. *J Anat* 230: 639–650, 2017.

Le Sant G, Nordez A, Hug F, Andrade R, Lecharte T, McNair P, Gross R. Effects of stroke injury on the shear modulus of the lower leg muscle during passive dorsiflexion. *J Appl Physiol* japplphysiol.00968.2017, 2018.

Winter, S. L. and Challis, J. H. The force-length curves of the human rectus femoris and gastrocnemius muscles in vivo. *J Appl Biomech* 26, 45–51, 2010.

Winter, D. A., Fuglevand, A. J. and Archer, S. E. Crosstalk in surface electromyography: Theoretical and practical estimates. *J. Electromyogr. Kinesiol.* 4, 15–26, 1994.

Xu J, Hug F, Fu SN. Stiffness of individual quadriceps muscle assessed using ultrasound SW elastography during passive stretching. *J Sport Heal Sci* 7: 245–249, 2016.

Yoshitake Y, Takai Y, Kanehisa H, Shinohara M. Muscle shear modulus measured with ultrasound shear-wave elastography across a wide range of contraction intensity. *Muscle and Nerve* 50: 103–113, 2014.

TABLE

Table 1. Architectural characteristics of target muscles | mean (SD)

Muscle	Optimal fascicle length (cm)		Pennation angle (deg)		PCSA (cm^2)
Biceps brachii	12.8 (3.2)*	NA	~0*	0.5 (0.0)§	3.1 (1.0)‡
Tibialis anterior	6.8 (0.8)†	NA	9.6 (3.1)†	7.7 (0.9)§	10.9 (3.0)†
Medial Gastrocnemius	5.1 (0.9)†	4.7 (1.1)§	9.9 (4.4)†	19.1 (1.4)§	21.1 (5.7)†

§ Present study (n=12), fascicle length and pennation angle with muscle at rest.
* Murray et al., 2000 (n=10)
‡ Veeger et al. 1997 (n=14)
† Ward et al., 2009 (TA: n=21, MG: n=20)

FIGURES AND CAPTIONS

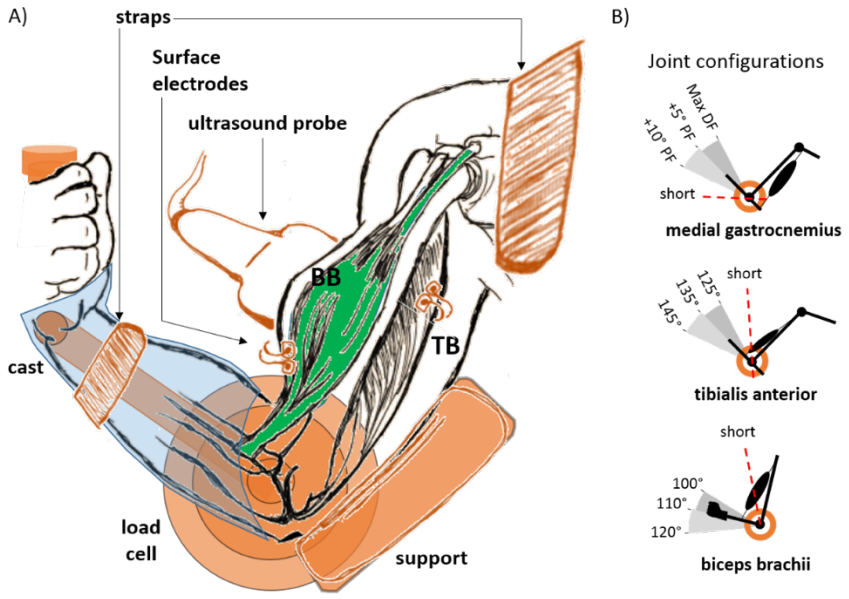

Figure 1. Schematic drawing of the experimental setup for measuring shear wave velocity (SWV), torque and activation on biceps brachii. The subject was secured to a Biodex chair by fixing shoulder joint to the chair and using a cast to fix the wrist to a load cell. Bipolar surface electrodes were placed on the target muscle (biceps brachii long head, green) and its main antagonist (triceps brachii). The ultrasound transducer was positioned on the mid-belly of the muscle, parallel to muscle fascicle direction. B) Different joint angle configurations were imposed for each of the three muscles, based on their specific physiological range of motion. An additional 'short' joint configuration corresponded to the smallest joint angle achievable in experimental conditions; this condition minimizes the effect of passive tension on shear wave measures. BB: biceps brachii; TB: triceps brachii; DF: dorsiflexion; PF: plantarflexion.

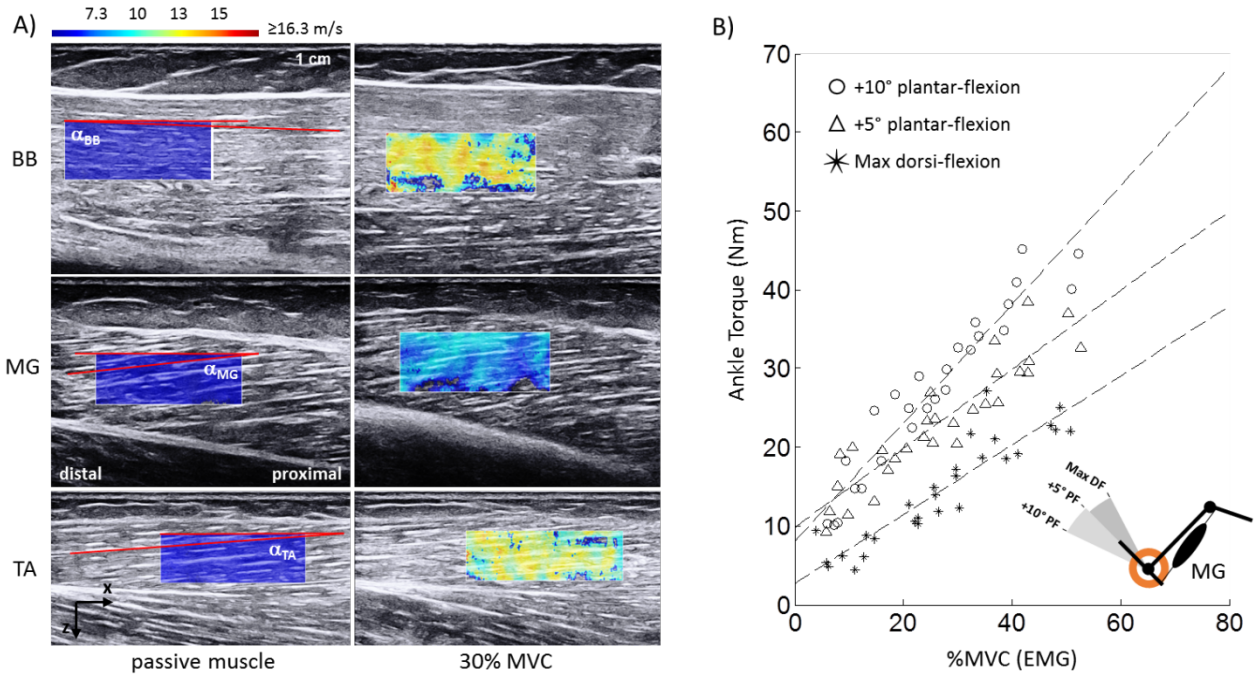

Figure 2. Ultrasound and torque data with different joint angle configurations and muscle activations. A) Heatmaps representing local shear wave velocity estimates on biceps brachii (BB), medial gastrocnemius (MG) and tibialis anterior (TA) for passive (left panels) and active muscle state (30% MVC, right panels). Red lines show an example of probe-fascicle angle measures (□) extracted for each muscle and condition. Note that MG heatmap shows qualitatively lower shear wave velocity, as calculated by the AIXplorer, compared to BB and TA at matching level of activation (30% MVC). B) Exemplar data of ankle torque measured in MG with increasing levels of activation and at three different joint angle configurations. Note that ankle torque covaried with muscle activation and its rate of change was different across ankle angles.

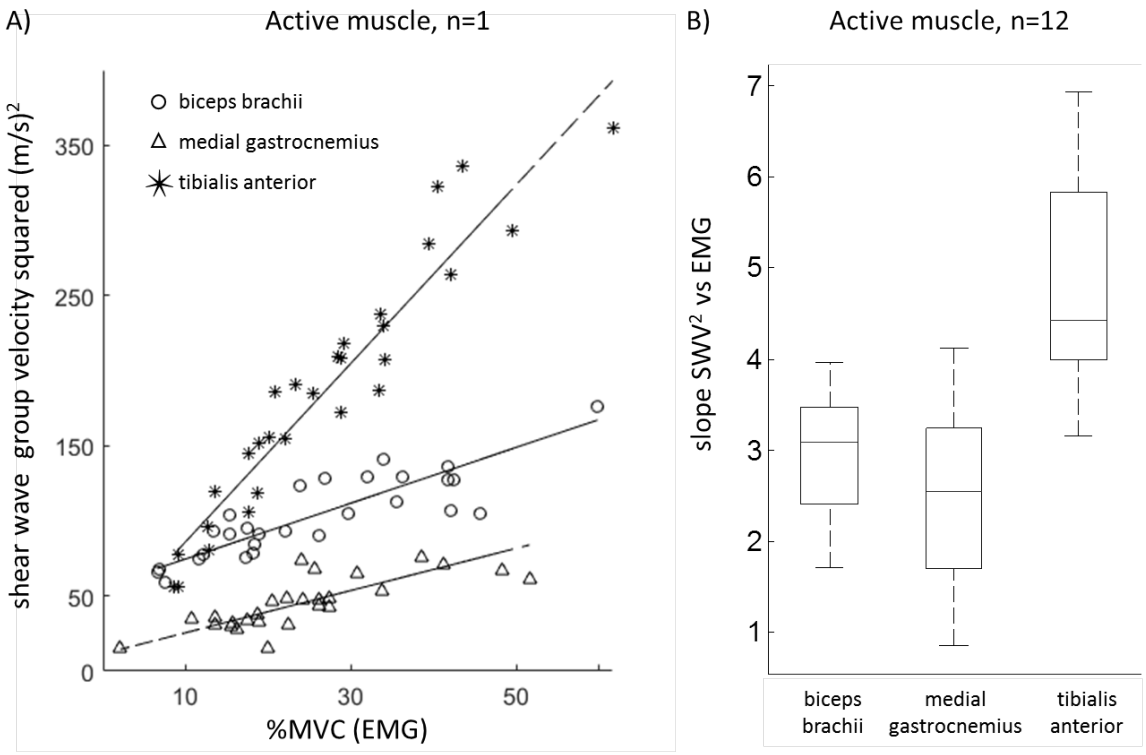

Figure 3. Variability of shear wave velocity measures across three different muscle types during isometric contraction. A) Exemplar data showing covariation of shear wave velocity squared (SWV^2) with muscle activation. A linear mixed-effects model was used to test for differences in the relationship between SWV^2 and activation across muscles. For this subject, slopes of the linear model are shown superimposed to experimental data. B) Median (midline), 75% and 25% percentile (box edges) for the slope of the linear model across subjects (n=12). Whiskers represent the most extreme slopes.

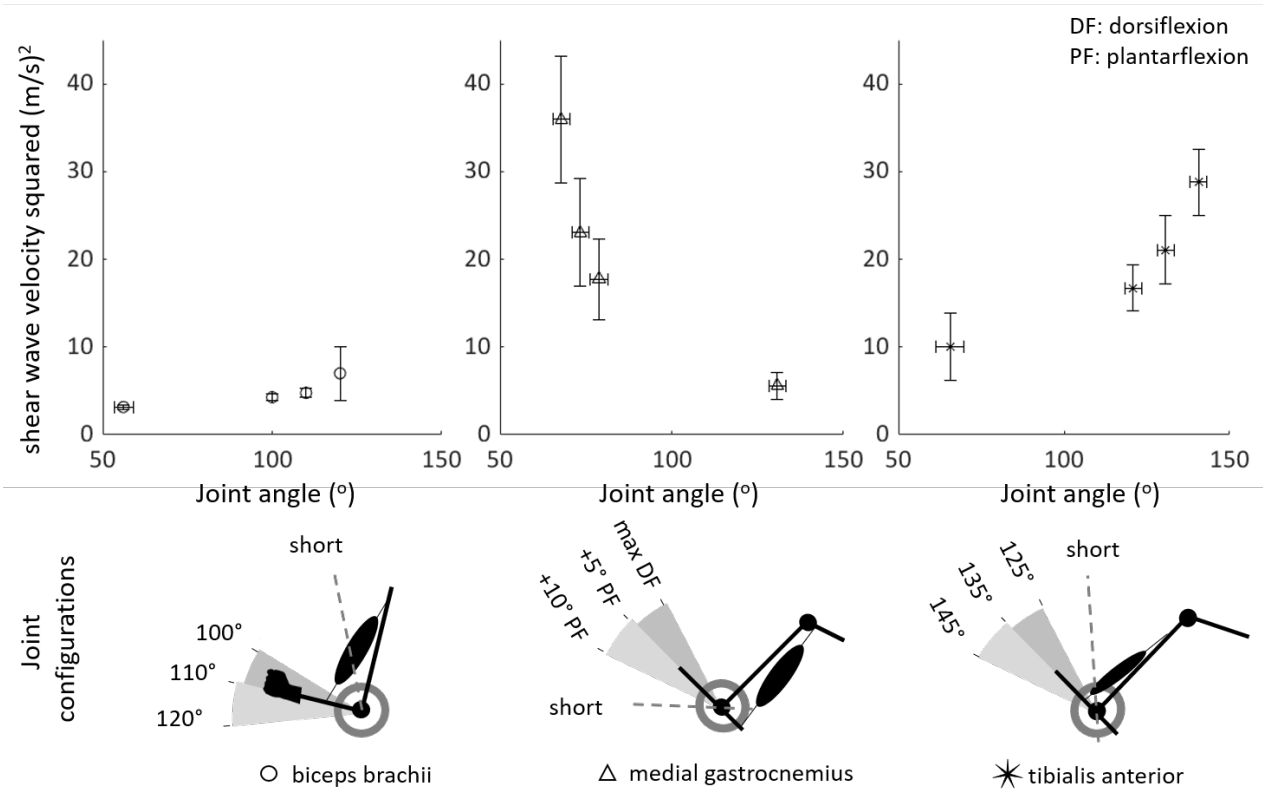

Figure 4. Dependency of shear wave velocity on passive muscle length across muscle types. A) Shear wave velocity squared (SWV^2) increased with lengthening the target muscles by imposing four different angles at the elbow and ankle. The 'short' condition, corresponding to the minimum measurable muscle length, shows differences in SWV^2 across muscles when the effect of passive tension is minimized. Repeated measures showed much lower variability in the biceps muscle (parallel) compared to tibialis (pennate) and gastrocnemius (highly pennate); mean ± SD, n = 12.

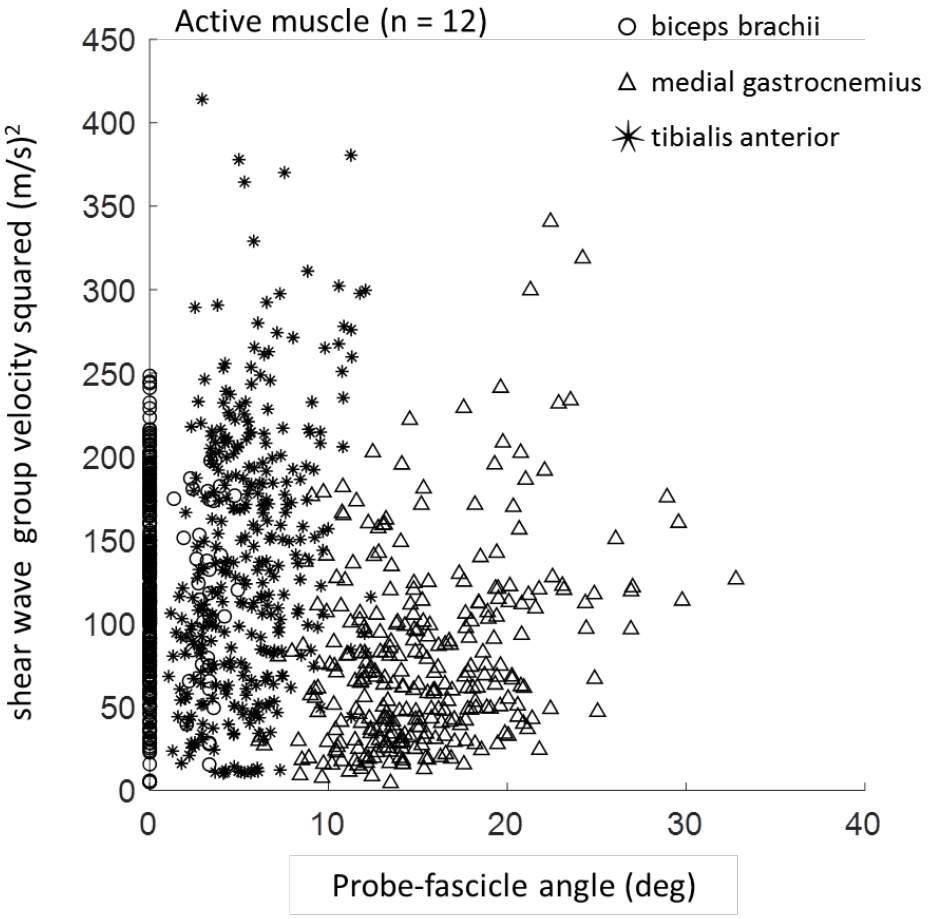

Figure 5. Effect of the angle between ultrasound transducer and fascicle orientation on SWV. Variation of SWV squared across different activation levels was partially associated with changes in the probe-fascicle angle in medial gastrocnemius (MG) and tibialis anterior (TA), while such angle was virtually zero for all applied conditions in biceps brachii (BB). The minimum probe-fascicle angle at 0 %MVC reflects the pennation angle for each muscle under passive conditions (mean ± SD, BB = 0.1 ± 0.43, MG = 12.1 ± 3.2, TA = 5.6 ± 1.9). Note that probe-fascicle angle will increase during activation due to pennation angle changes resulting from muscle contraction.